The effect of Pauli repulsion on the molecular exchange-correlation Kohn-Sham potential. A comparitive calculation of Ne2 and N2.

Gritsenko, O.V.; Schipper, P.R.T.; Baerends, E.J.

published in
Physical Review A. Atomic, Molecular and Optical Physics
1998

DOI (link to publisher)
10.1103/PhysRevA.57.3450

document version
Publisher's PDF, also known as Version of record

Effect of Pauli repulsion on the molecular exchange-correlation Kohn-Sham potential: A comparative calculation of Ne_2 and N_2

O. V. Gritsenko, P. R. T. Schipper, and E. J. Baerends
Scheikundig Laboratorium der Vrije Universiteit, De Boelelaan 1083, 1081 HV Amsterdam, The Netherlands
(Received 10 November 1997)

The Pauli repulsion between closed shells of two interacting systems induces structure in the exchange-correlation Kohn-Sham potential ν_{xc}. This effect has been studied by the construction of ν_{xc} from the *ab initio* correlated density ρ for the Ne_2 dimer. Pauli repulsion manifests itself in the formation of a characteristic bond midpoint peak of ν_{xc}. The behavior of ν_{xc} has been analyzed by means of a partitioning into various components: the potential of the exchange-correlation hole ν_{xc}^{hole}, the kinetic component $\nu_{c,kin}$, and the ''response'' component ν_{resp}. These components have been constructed from *ab initio* first- and second-order density matrices. All the components display bond midpoint peaks that contribute to the corresponding peak of ν_{xc}. The peaks of ν_{xc}^{hole} and $\nu_{c,kin}$ have been interpreted in terms of localization and mobility of the exchange-correlation hole, while the peak of ν_{resp} is related to the Pauli repulsion with the help of the approximation of Krieger-Li-Iafrate for this potential. The results obtained have been compared with those for the N_2 molecule. [S1050-2947(98)06505-6]

PACS number(s): 31.25.−v

I. INTRODUCTION

The Kohn-Sham (KS) approach of density-functional theory (DFT) provides an efficient description of electron exchange and correlation, since the local state-independent exchange-correlation potential $\nu_{xc}(\mathbf{r})$ incorporates all effects of electron correlation in the one-electron KS equations [1]

$$\left\{-\frac{1}{2}\nabla^2+\nu_{ext}(\mathbf{r})+\nu_H(\mathbf{r})+\nu_{xc}(\mathbf{r})\right\}\phi_i(\mathbf{r})=\varepsilon_i\phi_i(\mathbf{r})\,. \tag{1.1}$$

Other potentials in Eq. (1.1) are the external potential ν_{ext} and the Hartree potential ν_H of the electrostatic electron repulsion. Various effects of electron correlation are represented with the components of ν_{xc} according to the partition scheme of Refs. [2,3]:

$$\nu_{xc}(\mathbf{r})=\nu_{xc}^{hole}(\mathbf{r})+\nu_{c,kin}(\mathbf{r})+\nu_{resp}(\mathbf{r})\,. \tag{1.2}$$

The main correlation effect, the formation of the exchange-correlation hole around the reference electron at $\mathbf{r}$, is represented in Eq. (1.2) with the potential of the exchange-correlation hole ν_{xc}^{hole}, while the potential $\nu_{c,kin}$ represents the effect of Coulomb correlation on the kinetic functional and the potential ν_{resp} represents ''response'' effects on ν_{xc}^{hole} and $\nu_{c,kin}$. The potentials ν_{xc}^{hole} and $\nu_{c,kin}$ contribute also to the exchange-correlation energy density ε_{xc} defined in [4,5]

$$\varepsilon_{xc}(\mathbf{r})=\nu_{c,kin}(\mathbf{r})+\tfrac{1}{2}\nu_{xc}^{hole}(\mathbf{r}), \tag{1.3}$$

which directly yields the exchange-correlation energy E_{xc} of a many-electron system through the integral

$$E_{xc}=\int\rho(\mathbf{r})\varepsilon_{xc}(\mathbf{r})d\mathbf{r}. \tag{1.4}$$

In its turn, the potential ν_{xc} is defined as the functional derivative of E_{xc}:

$$\nu_{xc}([\rho];\mathbf{r})=\frac{\delta E_{xc}[\rho]}{\delta\rho(\mathbf{r})}. \tag{1.5}$$

Accurate functions $\nu_{xc}(\mathbf{r})$ and $\varepsilon_{xc}(\mathbf{r})$ can be obtained numerically from accurate *ab initio* wave functions. Examples of $\nu_{xc}(\mathbf{r})$ and $\varepsilon_{xc}(\mathbf{r})$ for atomic and prototype molecular systems representing the main types of bonding and nonbonding interactions can serve for the analysis of the effects of electron correlation and as benchmarks for the corresponding DFT approximations. The potentials ν_{xc} for the lightest many-electron closed-shell atoms Be and Ne were constructed with a variety of methods [6-13], while a systematic calculation of ν_{xc} for atoms Li through Ar was performed by the method of Zhao and Parr [11] in Refs. [14,15]. Molecular ν_{xc} potentials were constructed by the method of van Leeuwen and Baerends [13] for the hydrides LiH, BH, HF, CH_2 [16,5,17,18] and dimers Li_2, C_2, N_2, F_2 [19,20,18] and by the above-mentioned method of Zhao and Parr for a number of molecules in the papers of Handy *et al.* [21,22]. Examples of the correlation energy density ε_c for the He atom and the H_2 molecule were obtained in Ref. [4] followed by the examples of the exchange-correlation energy density ε_{xc} for LiH, BH, HF [5] and Li_2, N_2, F_2 [20].

Effects of electron correlation manifest themselves in characteristic features of ν_{xc}, ε_{xc} and their components. In particular, exchange interaction of electrons of atomic shells produces atomic intershell peaks of ν_{xc} [23–26] and the corresponding steps of ν_{resp} [3,27,28]. The left-right Coulomb correlation of valence electrons, a molecular correlation effect, produces a bond midpoint peak of $\nu_{c,kin}$ [2,29] and a positive buildup of the molecular ν_{xc} [30,31,17] and ν_{resp} [17] around the more electronegative atom.

In this paper the manifestation of another molecular effect, Pauli repulsion between closed electron shells of two interacting fragments, is investigated. The noble-gas dimer Ne_2 at a short interatomic distance R(Ne-Ne) has been chosen as a prototype system with Pauli repulsion. The poten-

tials $\nu_{xc}(\mathbf{r})$, $\nu_{xc}^{hole}(\mathbf{r})$, $\nu_{c,kin}(\mathbf{r})$, $\nu_{resp}(\mathbf{r})$ constructed for Ne_2 from an *ab initio* wave function using the configuration interaction (CI) method are compared with those obtained for the N_2 molecule, a typical system with strong covalent bonds. The difference in the form of the potentials $\nu_{xc}^{hole}(\mathbf{r})$ and $\nu_{c,kin}(\mathbf{r})$ for Ne_2 and N_2 is rationalized in terms of the different localization and mobility of the corresponding exchange-correlation holes. The effect of Pauli repulsion on the form of the response potential ν_{resp} is analyzed within the approximation of Krieger, Li, and Iafrate (KLI) [26] for this potential. As will be shown below, for Ne_2 Pauli repulsion creates characteristic bond midpoint peaks for all potentials considered.

II. PARTITIONING OF ν_{xc}

In this section we will present the definition of the potentials ν_{xc}^{hole}, $\nu_{c,kin}$, and ν_{resp}, the components (1.2) of the exchange-correlation potential ν_{xc}. The potential of the exchange-correlation hole ν_{xc}^{hole} is expressed through the partially integrated diagonal part of the second-order density matrix $\rho_2(\mathbf{r}_1,\mathbf{r}_2)$ or through the pair-correlation function $g^{\lambda}(\mathbf{r}_1,\mathbf{r}_2)$ with the electron interaction λ/r_{12} at full strength $\lambda=1$ and also through the exchange-correlation hole function $\rho_{xc}(\mathbf{r}_2|\mathbf{r}_1)$:

$$\nu_{xc}^{hole}(\mathbf{r}_1)=\int \frac{\rho_2(\mathbf{r}_1,\mathbf{r}_2)-\rho(\mathbf{r}_1)\rho(\mathbf{r}_2)}{|\mathbf{r}_1-\mathbf{r}_2|\rho(\mathbf{r}_1)}\,d\mathbf{r}_2$$
$$=\int \frac{\rho(\mathbf{r}_2)[g^{\lambda=1}(\mathbf{r}_1,\mathbf{r}_2)-1]}{|\mathbf{r}_1-\mathbf{r}_2|}\,d\mathbf{r}_2$$
$$=\int \frac{\rho_{xc}(\mathbf{r}_2|\mathbf{r}_1)}{|\mathbf{r}_1-\mathbf{r}_2|}\,d\mathbf{r}_2. \qquad (2.1)$$

As follows from Eq. (2.1), the value of ν_{xc}^{hole} at $\mathbf{r}_1$ is determined by the form of the exchange-correlation hole, i.e., by the form of ρ_{xc} as a function of $\mathbf{r}_2$.

The kinetic component $\nu_{c,kin}$ [2,5] is the kinetic correlation energy density,

$$T_c=T-T_s=\int \rho(\mathbf{r})[\nu_{kin}(\mathbf{r})-v_{s,kin}(\mathbf{r})]d\mathbf{r}$$
$$=\int \rho(\mathbf{r})\nu_{c,kin}(\mathbf{r})d\mathbf{r}, \qquad (2.2)$$

which can be defined via the conditional probability amplitudes [32] $\Phi(s_1,\mathbf{x}_2,\ldots,\mathbf{x}_N|\mathbf{r}_1)$ and $\Phi_s(s_1,\mathbf{x}_2,\ldots,\mathbf{x}_N|\mathbf{r}_1)$ of the total ground-state wave function $\Psi_0(\mathbf{x}_1,\mathbf{x}_2,\ldots,\mathbf{x}_N)$ and the Kohn-Sham determinant $\Psi_s(\mathbf{x}_1,\mathbf{x}_2,\ldots,\mathbf{x}_N)$ ($\{\mathbf{x}_i\}=\{\mathbf{r}_i,s_i\}$, $\{\mathbf{r}_i\}$ are the space and $\{s_i\}$ are the spin variables) and it can be expressed through the first-order density matrices

$$\Phi(s_1,\mathbf{x}_2,\ldots,\mathbf{x}_N|\mathbf{r}_1)=\frac{\Psi_0(\mathbf{x}_1,\mathbf{x}_2,\ldots,\mathbf{x}_N)}{\sqrt{\rho(\mathbf{r}_1)/N}}, \qquad (2.3)$$

$$\Phi_s(s_1,\mathbf{x}_2,\ldots,\mathbf{x}_N|\mathbf{r}_1)=\frac{\Psi_s(\mathbf{x}_1,\mathbf{x}_2,\ldots,\mathbf{x}_N)}{\sqrt{\rho(\mathbf{r}_1)/N}}, \qquad (2.4)$$

$$\nu_{c,kin}(\mathbf{r}_1)=\frac{1}{2}\int |\nabla_1\Phi(s_1,\mathbf{x}_2,\ldots,\mathbf{x}_N|\mathbf{r}_1)|^2 ds_1 d\mathbf{x}_2\cdots d\mathbf{x}_N$$
$$-\frac{1}{2}\int |\nabla_1\Phi_s(s_1,\mathbf{x}_2,\ldots,\mathbf{x}_N|\mathbf{r}_1)|^2 ds_1 d\mathbf{x}_2\cdots d\mathbf{x}_N$$
$$=\frac{\nabla_1\cdot\nabla_1[\rho(\mathbf{r}_1',\mathbf{r}_1)-\rho_s(\mathbf{r}_1',\mathbf{r}_1)]|_{\mathbf{r}_1'=\mathbf{r}_1}}{2\rho(\mathbf{r}_1)}. \qquad (2.5)$$

$\nu_{c,kin}$ is here obtained from first derivatives of the one-electron density matrices. It can obviously, as a difference of kinetic energy densities, also be obtained in terms of second derivatives of one-electron density matrices. Because $\nu_{c,kin}$ is a unique function of position, the two alternative expressions yield the same local values [2,20]. ν_{kin} is a measure of the magnitude of change in Φ, i.e., a change in the total exchange-correlation hole, with changing $\mathbf{r}_1$. It peaks when this hole changes rapidly with changing $\mathbf{r}_1$. Similarly $\nu_{s,kin}$ reflects the magnitude of change in Φ_s with changing $\mathbf{r}_1$, i.e., change in the exchange-only (Fermi) hole. $\nu_{c,kin}$ thus reflects the differential effect, basically the mobility of the correlation (Coulomb) hole with variations of the reference position $\mathbf{r}_1$.

The last component of (1.2), the response potential ν_{resp} is defined as follows:

$$\nu_{resp}(\mathbf{r}_3)=\frac{1}{2}\int \frac{\rho(\mathbf{r}_1)\rho(\mathbf{r}_2)}{|\mathbf{r}_1-\mathbf{r}_2|}\frac{\delta_g^{\lambda=1}([\rho];\mathbf{r}_1,\mathbf{r}_2)}{\delta\rho(\mathbf{r}_3)}\,d\mathbf{r}_1 d\mathbf{r}_2$$
$$+\int \rho(\mathbf{r}_2)\frac{\delta\nu_{c,kin}([\rho];\mathbf{r}_2)}{\delta\rho(\mathbf{r}_3)}\,d\mathbf{r}_2. \qquad (2.6)$$

As shown in [2], ν_{resp} can be expressed also via the expectation values of the Hamiltonian of the $(N-1)$-electron system calculated with the conditional probability amplitudes Φ and Φ_s of Eqs. (2.3) and (2.4). Note that ν_{resp} is, compared to other components of Eq. (1.2), a somewhat peculiar potential. While the ν_{xc}^{hole} and $\nu_{c,kin}$ potentials contribute also to the exchange-correlation energy density ε_{xc} [Eq. (1.3)], ν_{resp} only enters ν_{xc} and it does not contribute to ε_{xc}, thus representing the ''nonenergy'' component of ν_{xc}. The potentials ν_{xc}^{hole} and $\nu_{c,kin}$ are expressed in a simple way through the second- and first-order density matrices, while ν_{resp} lacks such a simple expression, which hampers its analysis. As a matter of fact, in order to obtain ν_{resp}, one has to construct the total exchange-correlation potential ν_{xc} and its components ν_{xc}^{hole} and $\nu_{c,kin}$ and then calculate ν_{resp} as the difference $\nu_{resp}=\nu_{xc}-\nu_{xc}^{hole}-\nu_{c,kin}$.

In the next section we shall analyze qualitatively the effect of Pauli repulsion on ν_{resp} using the approximation of Krieger, Li, and Iafrate ν_{resp}^{KLI} for this potential. ν_{resp}^{KLI} is a part of the KLI exchange potential ν_x^{KLI} [33]:

$$\nu_x^{KLI}(\mathbf{r})=\nu_x^{hole}(\mathbf{r})+\nu_{resp}^{KLI}(\mathbf{r}). \qquad (2.7)$$

ν_x^{KLI} models the exchange potential ν_x^{OPM} of the optimized potential model (OPM) [23,34,35]. One can also consider ν_x^{KLI} as an approximation to the exchange-correlation potential ν_{xc} of Eq. (1.2). In this approximation the kinetic contribution $\nu_{c,kin}$ due to Coulomb correlation is neglected, the

potential of the exchange-correlation hole ν_{xc}^{hole} is replaced with the potential of the exchange hole ν_x^{hole}, both ν_x^{hole} and the KLI response potential ν_{resp}^{KLI} being expressed in terms of the orbitals ϕ_i (a closed-shell system is considered):

$$\nu_x^{hole}(\mathbf{r}) = \sum_{i=1}^{N/2} \nu_{xi}(\mathbf{r}) \frac{2|\phi_i(\mathbf{r})|^2}{\rho(\mathbf{r})}, \tag{2.8}$$

$$\nu_{xi}(\mathbf{r}_1) = -\frac{1}{\phi_i(\mathbf{r}_1)} \sum_{j=1}^{N/2} \phi_j(\mathbf{r}_1) \int \frac{\phi_i(\mathbf{r}_2)\phi_j^*(\mathbf{r}_2)}{|\mathbf{r}_1-\mathbf{r}_2|} d\mathbf{r}_2, \tag{2.9}$$

$$\nu_{resp}^{KLI}(\mathbf{r}) = \sum_{i=1}^{N/2-1} w_i \frac{2|\phi_i(\mathbf{r})|^2}{\rho(\mathbf{r})}, \tag{2.10}$$

$$w_i = \int |\phi_i(\mathbf{r})|^2 [\nu_x^{KLI}(\mathbf{r}) - \nu_{xi}(\mathbf{r})] d\mathbf{r}. \tag{2.11}$$

According to Eq. (2.8), ν_x^{hole} is the statistical average of the Hartree-Fock exchange operators ν_{xi} of all occupied orbitals, while the expression (2.10) for ν_{resp}^{KLI} is the average of the orbital constants w_i, which does not include a contribution from the highest occupied molecular orbital (HOMO).

It follows from Eq. (2.10) that the form of ν_{resp}^{KLI} as a function of $\mathbf{r}$ is determined by the form of the KS orbitals $\phi_i(\mathbf{r})$ and density $\rho(\mathbf{r})$, and also by the relative magnitude of the orbital constants w_i. Since Pauli repulsion originates from the electron exchange, one can expect that the KLI approximation (2.10) reproduces (at least qualitatively) the Pauli repulsion effect on ν_{resp} of Eq. (2.6).

III. NOTION OF PAULI REPULSION AND CALCULATIONAL DETAILS

Pauli repulsion between closed shells is a manifestation of the Pauli exclusion principle, which is, in its turn, a consequence of the antisymmetry of a many-electron wave function. According to this principle, there is zero probability for two electrons to occupy the same point in the configurational space. This means that two electrons with the same spin have zero probability of being found at the same point in three-dimensional physical space.

Within the one-electron approach the exclusion principle requires that no two electrons occupy the same spin orbital. In particular, for the case of two interacting subsystems with closed electron shells the exclusion principle requires occupation of the antibonding molecular orbitals (MOs) of the total system, since in this case the number of electrons is always larger than the number of the available bonding spin orbitals. This gives rise to Pauli repulsion of the closed electron shells.

Pauli repulsion manifests itself in the depletion of the electron density ρ of the total system in the region of overlap of the densities of the closed-shell fragments. This can be illustrated with a two-orbital model applied to the simplest molecular closed-shell system, the He_2 dimer. In this case individual He atoms are represented with the s-type KS orbitals $a(\mathbf{r})$ and $b(\mathbf{r})$, while both bonding

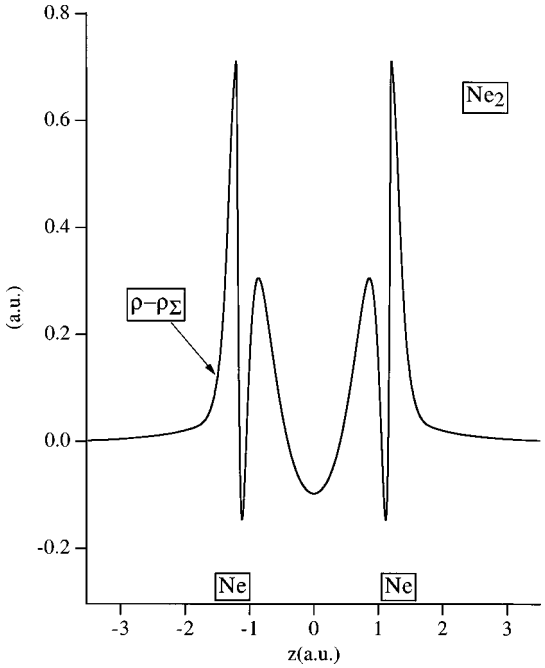

FIG. 1. Density redistribution $(\rho-\rho_\Sigma)$ along the bond axis for the Ne_2 dimer.

$$g(\mathbf{r}) = \frac{1}{\sqrt{2+2S}} [a(\mathbf{r}) + b(\mathbf{r})] \tag{3.1}$$

and antibonding

$$u(\mathbf{r}) = \frac{1}{\sqrt{2-2S}} [a(\mathbf{r}) - b(\mathbf{r})] \tag{3.2}$$

MOs $g(\mathbf{r})$ and $u(\mathbf{r})$ contribute to the molecular density ρ,

$$\rho(\mathbf{r}) = g^2(\mathbf{r}) + u^2(\mathbf{r}) = \frac{1}{1-S^2} [a^2(\mathbf{r}) + b^2(\mathbf{r}) - 2Sa(\mathbf{r})b(\mathbf{r})]. \tag{3.3}$$

In Eqs. (3.1)–(3.3) S is the overlap integral,

$$S = \int a(\mathbf{r})b(\mathbf{r})d\mathbf{r}. \tag{3.4}$$

One can see the effect of Pauli repulsion on ρ comparing Eq. (3.3) with the sum of atomic densities ρ_Σ:

$$\rho_\Sigma(\mathbf{r}) = a^2(\mathbf{r}) + b^2(\mathbf{r}). \tag{3.5}$$

ρ of Eq. (3.3) exhibits an electron charge depletion in the overlap region and a charge accumulation in the regions around the nuclei as compared to ρ_Σ [36]. Figure 1 illustrates these features of the density redistribution $(\rho-\rho_\Sigma)$ along the bond axis obtained with *ab initio* CI calculation for the Ne_2 dimer with a short interatomic distance $R(\text{Ne-Ne}) = 2.4$ bohrs. Apart from the charge rearrangements indicated above, there is in addition a sharp dip in $(\rho-\rho_\Sigma)$ practically at the nuclei. This is caused by the orthogonality requirement of the occupied valence shells $(2s,2p)$ on atom B onto the $1s$ shell of atom A, and vice versa. This is in fact also a

manifestation of Pauli repulsion, this time of core-valence type, which we will not further consider.

As shown in [36], the charge depletion leads to an increase of the kinetic energy, the principal energy effect of the Pauli repulsion. Pauli repulsion plays an important role, since the combined effect of covalent or ionic bonding of valence electrons and Pauli repulsion of the closed atomic subshells determines the equilibrium geometry of molecules. However, the effect of Pauli repulsion on the exchange-correlation potential ν_{xc} has not been studied yet.

In this paper, in order to study this effect, the potential ν_{xc} with its components ν_{xc}^{hole}, $\nu_{c,kin}$, and ν_{resp} has been constructed for the noble-gas dimer Ne_2. This system has been chosen, since at short interatomic distances it lacks bonding, thus representing the pure effect of Pauli repulsion of the closed $2s$ and $2p$ subshells of the Ne atoms. The potentials are compared with those constructed for the N_2 molecule, a prototype system with strong covalent bonds. *Ab initio* CI calculations of Ne_2 and N_2, with subsequent construction of the potentials, were performed at the bond distance $R(A\text{-}A)=2.074$ bohrs and at several larger distances using the ATMOL package [37]. For N_2 $R(A-A)=2.074$ bohrs is the equilibrium bond distance R_e, while for Ne_2 it is a short interatomic contact with a strong Pauli repulsion.

Having its origin in the exchange of electrons, the Pauli repulsion effect should not depend much on the amount of Coulomb correlation included in the CI calculation. Bearing this in mind, we have performed moderate size, single reference CI calculations for Ne_2 in a basis of six s-, five p-, and two d-contracted Gaussian functions, which has been obtained from the correlation-consistent polarized core-valence triple zeta added (cc-pCVTZ) basis [38]. However, for N_2 it becomes crucially important to properly take into account the Coulomb correlation of the electrons of the multiple bonds. Therefore, multireference CI (MRCI) calculations have been carried out for N_2 in the cc-pCVTZ basis. 106 reference configurations were selected within the internal space of 10 lowest-energy Hartree-Fock MOs. All single and double excitations from each reference configuration to either internal or external subspaces have been included in the MRCI, which have also been augmented with the configurations obtained by single excitation from a reference configuration to the internal subspace with subsequent single excitation to the external subspace. The MRCI calculation performed at R_e recovered 86% of the total Coulomb correlation energy for N_2.

To construct ν_{xc} and its components, the first-order density matrix $\rho(\mathbf{r}_1',\mathbf{r}_1)$, its diagonal part $\rho(\mathbf{r})$, and the diagonal part $\rho_2(\mathbf{r}_1,\mathbf{r}_2)$ of the second-order density matrix have been calculated from the CI wave function by means of a Gaussian orbital density functional code [2,39] based on the ATMOL package. The KS orbitals and potential have been constructed with the iterative procedure of van Leeuwen and Baerends [13] in the same basis of MOs as has been used for the CI calculations. The accuracy of the resultant KS solution can be characterized by the integrated difference between the calculated (from the KS orbitals) density ρ^m and target CI density ρ (absolute error of the iterative procedure)

$$\Delta\rho=\int |\rho^m(\mathbf{r})-\rho(\mathbf{r})|\,d\mathbf{r} \tag{3.6}$$

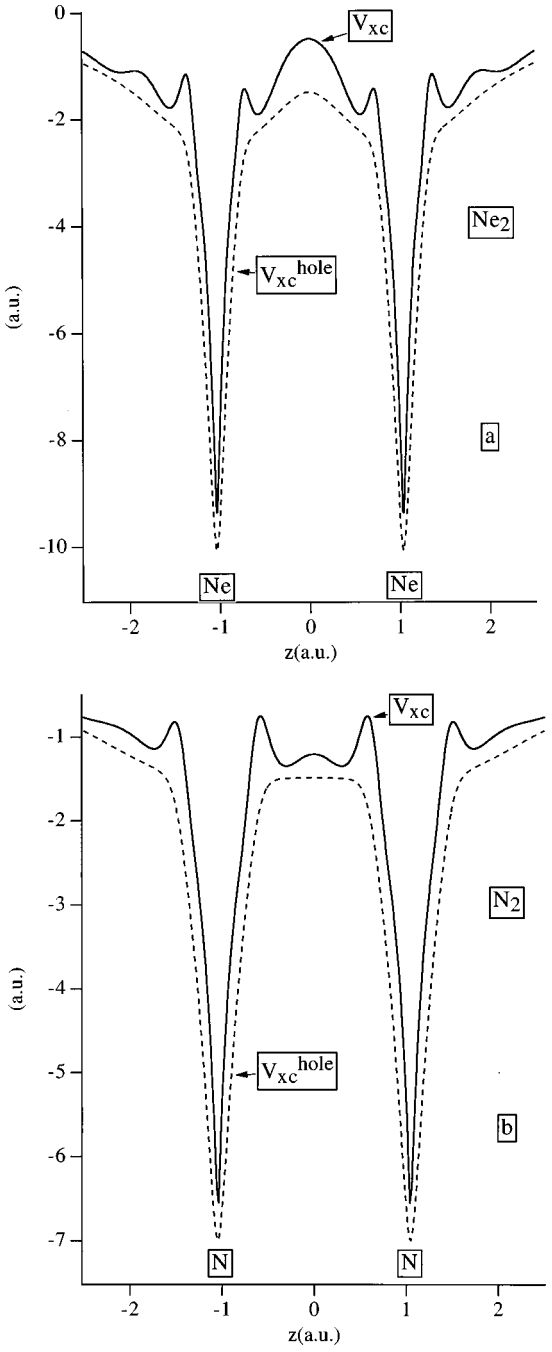

FIG. 2. The exchange-correlation potential ν_{xc} and the potential of the exchange-correlation hole ν_{xc}^{hole} along the bond axis (a) Ne_2 and (b) Ne_2.

with a typical value $\Delta\rho=0.003e$ for both Ne_2 and N_2.

IV. THE POTENTIALS FOR Ne_2 and N_2

Figure 2 compares the exchange-correlation potentials ν_{xc} and the potentials of the exchange-correlation hole ν_{xc}^{hole} constructed for Ne_2 and N_2 at the same bond distance $R(A\text{-}A)=2.074$ bohrs. The potentials are plotted along the bond axis as functions of the distance z from the bond midpoint, so that the pictures compare the region of the σ bond of N_2 with the region of the strong Pauli repulsion of the

occupied $2s$ and $2p_z$ orbitals of the individual Ne atoms of Ne_2.

In spite of this difference in the bonding patterns, the potentials ν_{xc} for these systems have similar qualitative features. For both systems ν_{xc} has deep wells around the nuclei, which represent, mainly, the attractive effect of the contracted Fermi hole, similar to the $1s$ charge density, that exists around a reference electron in the $1s$ shell, accounting for the excluded self-interaction of $1s$ electrons. These wells are terminated with intershell peaks between the core and valence regions of atoms Ne and N. In the bonding region ν_{xc} displays a bond midpoint peak. However, there is a significant quantitative difference here. While for N_2 this peak is relatively small, ν_{xc} for Ne_2 possesses a high bond midpoint peak approaching zero value at $z=0$ [compare Figs. 2(a) and 2(b)]. In order to find out the reasons for this difference, we shall compare the components (1.2) of ν_{xc}.

(a) The hole potential ν_{xc}^{hole}. Comparison of the main components, the hole potentials ν_{xc}^{hole} of Ne_2 and N_2 reveals a striking difference in the bonding region (small z values). For N_2 ν_{xc}^{hole} has a plateau in this region [see Fig. 2(b)], while for Ne_2 it forms a bond midpoint peak [see Fig. 2(a)], which contributes to the corresponding peak of ν_{xc}.

A possible interpretation of this difference can be based on the different form of the exchange-correlation hole functions $\rho_{xc}(\mathbf{r}_2|\mathbf{r}_1)$ of Ne_2 and N_2, the latter function, according to Eq. (2.1), determining the value of $\nu_{xc}^{hole}(\mathbf{r}_1)$. In the case of the N_2 molecule the region around the bond midpoint is the interior region of the exchange (Fermi) hole of the σ bond, which is delocalized symmetrically over both N atoms [40]. The hole has large depth around each nucleus and it is essentially static; i.e., it does not change shape when the reference position is changed around the bond midpoint [40]. In [20], in order to make a qualitative interpretation of the plateau form of ν_{xc}^{hole}, this hole was approximated effectively with a simple electrostatic model of two charges of $-0.5e$, which are placed along the bond axis at distances r and $-r$ from the bond midpoint. This model is valid for small displacements z from the bond midpoint and produces the following very simple hole potential:

$$\nu_{mod}^{hole}(z)=-\frac{0.5}{r-z}-\frac{0.5}{r+z}\cong-\frac{1}{r}\left(1-\frac{z^2}{r^2}\right). \qquad (4.1)$$

Within this model the potential will only change in second order for small displacements ($z/r\ll 1$) from the bond midpoint, so that it is essentially flat around the bond midpoint. These simple electrostatic arguments show that the plateau of ν_{xc}^{hole} in the bonding region of N_2 [see Fig. 2(b)] can be understood as a manifestation of the delocalized, static nature of the corresponding Fermi hole. The presence of the additional Coulomb hole, which at R_e is much weaker than the exchange hole, does not change this feature qualitatively.

When not only the bonding orbital is occupied, but also the corresponding antibonding orbital, the Fermi hole behaves very differently. In this case, an orbital localization procedure will give two localized orbitals around the two atoms. The Fermi hole is similar to minus the charge density of the localized orbital when the reference electron is somewhere within the region of the localized orbital [41,42]. When the reference electron moves from a nucleus towards the bond midpoint, the hole will first remain localized in the atomic region and the potential will have a Coulombic behavior when the midpoint is approached. However, when the reference electron crosses the bond midpoint, it will enter the region of the localized orbital around the other nucleus, and the hole will accordingly rapidly change shape and become centered around the other nucleus. Taken together, two symmetrical Coulombic segments form the bond midpoint peak of ν_{xc}^{hole} [see Fig. 2(a)]. The ''jumping'' of the Fermi hole when the reference position crosses the bond midpoint can be deduced immediately from the Fermi amplitude $\varphi^{Fermi}(\mathbf{r}_2|\mathbf{r}_1)$, where $-|\varphi^{Fermi}(\mathbf{r}_2|\mathbf{r}_1)|^2$ describes the hole as a function of position $\mathbf{r}_2$ when the reference electron is at $\mathbf{r}_1$. Using φ_1 and φ_2 for the bonding and antibonding orbitals g and u, respectively, the exact expression for the Fermi amplitude is [40]

$$\varphi^{Fermi}(\mathbf{r}_2|\mathbf{r}_1)=\sum_{i=1}^{2} c^{Fermi}(\mathbf{r}_1)\varphi_i(\mathbf{r}_2)=\sum_{i=1}^{2}\frac{\sqrt{2}\varphi_i(\mathbf{r}_1)}{\sqrt{\rho(\mathbf{r}_1)}}\varphi_i(\mathbf{r}_2). \qquad (4.2)$$

The amplitude is a linear combination of the occupied orbitals, with coefficients that are dependent on the reference position. With $\mathbf{r}_1$ around atom A, both $g(\mathbf{r}_1)$ and $u(\mathbf{r}_1)$ are approximately $+(1/2)\sqrt{\rho}(\mathbf{r}_1)$, and the amplitude (as a function of $\mathbf{r}_2$) has shape $\sim a(\mathbf{r}_2)$, and $\rho_x(\mathbf{r}_2|\mathbf{r}_1)=-|a(\mathbf{r}_2)|^2$ is localized at atom A. If, however, $\mathbf{r}_1$ is around atom B, $u(\mathbf{r}_1)=-g(\mathbf{r}_1)\approx+(1/2)\sqrt{\rho}(\mathbf{r}_1)$, the Fermi amplitude becomes $\sim b(\mathbf{r}_2)$, and the hole $\rho_x(\mathbf{r}_2|\mathbf{r}_1)\approx-|b(\mathbf{r}_2)|^2$ is localized at atom B.

(b) The kinetic correlation potential $\nu_{c,kin}$. When the exchange hole makes a ''jump,'' i.e., changes rapidly over a short $\mathbf{r}_1$ interval, both $\nu_{s,kin}$ and ν_{kin} will exhibit a peak. This has been observed when $\mathbf{r}_1$ crosses an intershell boundary in an atom [2,3]. According to the analysis above, in the case of Ne_2 we may expect such peaks in $\nu_{s,kin}$ and ν_{kin} at the bond midpoint. In $\nu_{c,kin}$ these cancel, and the observed small but clearly visible bond midpoint peak of the potential $\nu_{c,kin}$ in Ne_2 (see Fig. 3) reflects the mobility of just the Coulomb correlation hole near $z=0$.

The bond midpoint peak of $\nu_{c,kin}$ for Ne_2 resembles the positive maximum in $\nu_{c,kin}$ at the bond midpoint for the H_2 molecule, which was established in Ref. [2]. This maximum becomes a very striking peak in $\nu_{c,kin}$ in stretched H_2. However, the $\nu_{c,kin}$ peaks represent different kinetic correlation effects in the cases of H_2 and Ne_2. The peak for Ne_2 arises in a no-bond situation and represents a ''jump'' of the essentially localized atomic Coulomb hole from one atom to another. For H_2 on the other hand the positive maximum of $\nu_{c,kin}$ arises in an electron pair bond where the Coulomb hole is delocalized over both atoms, being negative on the atom nearest to the reference position and positive on the other atom. The positive maximum of $\nu_{c,kin}$ reflects in this case the rapid reversal in sign of the Coulomb hole when the reference position passes the bond midpoint (cf. [40,43]), the hole remaining delocalized. For stretched H_2 the Coulomb hole becomes large and the hole switching when $\mathbf{r}_1$ passes the bond midpoint induces a much larger peak than at equilibrium bond length. In the present case of three electron pair

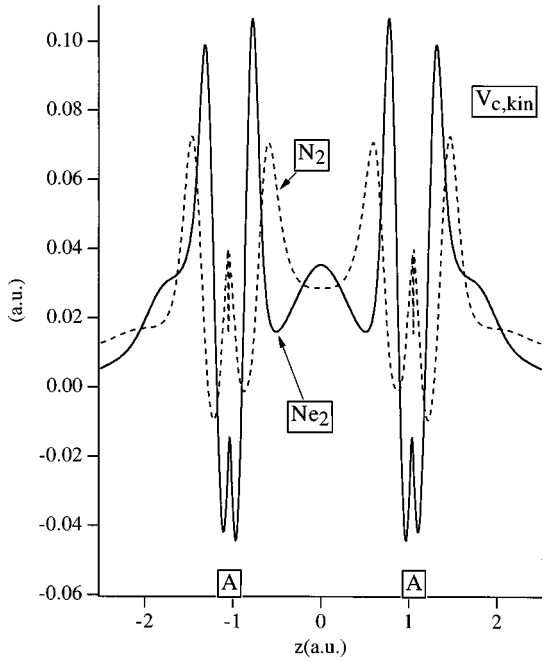

FIG. 3. Comparison of the potentials $\nu_{c,\mathrm{kin}}$ for Ne_2 and N_2.

bonds in N_2 at equilibrium distance, we find that $\nu_{c,\mathrm{kin}}$ is positive around the bond midpoint (see Fig. 3), in agreement with expectations [2,20], although it does not exhibit a peak but rather a valley. For both Ne_2 and N_2 the most visible features of $\nu_{c,\mathrm{kin}}$ are the $1s$-$2s$ intershell peaks and the peaks at small distances to the nuclei analogous to the peaks observed and explained in Refs. [16,5] for the hydrides LiH, BH, and HF.

(c) The response potential ν_{resp}. In Fig. 4 the potentials ν_{resp} are compared for Ne_2 and N_2. A spectacular manifestation of the strong Pauli repulsion is the relatively large bond midpoint peak of the potential ν_{resp} for Ne_2 (see Fig. 4). The

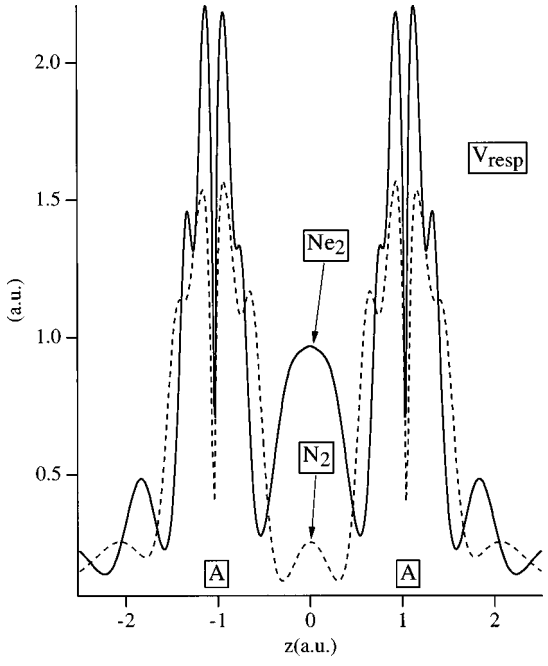

FIG. 4. Comparison of the potentials ν_{resp} for Ne_2 and N_2.

height of this peak is much larger than that of the corresponding peak of the potential $\nu_{c,\mathrm{kin}}$ and it is ν_{resp} that is responsible for the buildup of the additional bond midpoint peak of the total exchange-correlation potential ν_{xc} on top of the peak of its component $\nu_{\mathrm{xc}}^{\mathrm{hole}}$ [see Fig. 2(a)].

Before analyzing this bond midpoint peak more closely, we note that another characteristic feature of ν_{resp} is its steplike high buildups in the atomic core regions, which were established and interpreted in [3,28]. The typical height of the core step $\Delta\nu_{\mathrm{resp}}$ for N_2 is smaller than that for Ne_2 and it is in agreement with its rough estimate [27] for the case of the exchange-only potential ν_x of the optimized potential model (OPM):

$$\Delta\nu_{\mathrm{resp}} \approx 0.38\sqrt{\varepsilon_{\mathrm{HOMO}}-\varepsilon_i}, \tag{4.3}$$

where in this case ε_i is the energy of the core orbital. The step pattern of ν_{resp} is disturbed by cusps and wiggles near the nucleus, which we have not further analyzed.

We have observed before [3,28] that the step pattern in the atomic shells can be related to the ''jumping'' of the exchange hole when the reference position moves across the intershell boundaries and that this behaviour is already represented by the KLI approximation for the response part of the exchange potential, $\nu_{x,\mathrm{resp}}^{\mathrm{KLI}}$, Eq. (2.10). The bond midpoint peak of ν_{resp} can also be related qualitatively to the Pauli repulsion and the concomitant jumping of the exchange hole from one atom to the next with the help of the KLI model $\nu_{\mathrm{resp}}^{\mathrm{KLI}}$ [Eq. (2.10)]. We consider the simplest closed-shell system with Pauli repulsion, the He_2 dimer, with the two occupied KS MOs $g(\mathbf{r})$ and $u(\mathbf{r})$ mentioned before. It follows from Eq. (2.10) that $\nu_{\mathrm{resp}}^{\mathrm{KLI}}$ for He_2 contains only one term:

$$\nu_{\mathrm{resp}}^{\mathrm{KLI}}(\mathbf{r}) = w_g \frac{2|g(\mathbf{r})|^2}{2|g(\mathbf{r})|^2+2|u(\mathbf{r})|^2}. \tag{4.4}$$

The form of $\nu_{\mathrm{resp}}^{\mathrm{KLI}}$ as a function of the electron coordinate $\mathbf{r}$ is determined by the ratio $|g(\mathbf{r})|^2/[|g(\mathbf{r})|^2+|u(\mathbf{r})|^2]$. The ratio attains a maximum value 1.0 at the bond midpoint plane, since the antibonding orbital $u(\mathbf{r})$ has a zero value at this plane. In particular when the overlap S [Eq. (3.4)] is large, the value of $u(\mathbf{r})$ will be significantly larger in the atomic regions than that of $g(\mathbf{r})$ due to the different factors $1/\sqrt{(2-2S)}$ and $1/\sqrt{(2+2S)}$ [Eqs. (3.1) and (3.2)], respectively. The ratio $|g(\mathbf{r})|^2/[|g(\mathbf{r})|^2+|u(\mathbf{r})|^2]$ will then rapidly decrease to a value well below 0.5 for positions off the bond midplane. At large distances from the nuclei a more diffuse orbital $u(\mathbf{r})$ brings a dominant contribution to the density ρ and the ratio approaches the zero value. Thus, the potential $\nu_{\mathrm{resp}}^{\mathrm{KLI}}$ develops a peak of height w_g at the bond midpoint that originates from the occupation of the antibonding MO, so that it can be considered as the Pauli repulsion effect.

Formula (4.4) is also approximately valid for the potential $\nu_{\mathrm{resp}}^{\mathrm{KLI}}$ of the Ne_2 molecule in the region around the bond midpoint, if we neglect contributions from all orbitals but the antibonding HOMO $u(\mathbf{r})=2p_{\sigma u}$ and the corresponding bonding MO $g(\mathbf{r})=2p_{\sigma g}$. In this case we consider only Pauli repulsion of the occupied $2p_z$ orbitals of two Ne atoms, which, according to Eq. (4.4), creates the bond midpoint

peak of ν_{resp}^{KLI}. The interaction of the closed $2s$ subshells of Ne atoms adds an additional Pauli repulsion effect at the bond midpoint.

It is interesting to note that the potential ν_{resp} constructed for the N_2 molecule also displays a bond midpoint peak, though it is much smaller than that for Ne_2. We conjecture that this peak represents Pauli repulsion of the closed $2s$ subshells of N atoms, which has indeed been shown to play an important role in the electron momentum density [44]. We note that, in agreement with this assignment, for both N_2 and Ne_2 the height of the peak of the constructed potential ν_{resp} decreases with increasing bond distance, which correlates with the decreasing Pauli repulsion of the closed electron shells. The peak of ν_{resp} for N_2 is responsible for the same feature in ν_{xc} [compare Figs. 2(b) and 4].

V. CONCLUSIONS

In this paper the effect of Pauli repulsion between closed shells on the exchange-correlation Kohn-Sham potential ν_{xc} has been established and analyzed. ν_{xc} and its components have been constructed from *ab initio* correlated first- and second-order density matrices for the Ne_2 dimer at short interatomic distances, a prototype system with strong Pauli repulsion. The results have been compared with those for the N_2 molecule, a prototype system with strong covalent bonding.

Pauli repulsion manifests itself in the formation of a characteristic bond midpoint peak of ν_{xc}. This peak is built up primarily by corresponding peaks in the hole and response parts of the potential, $\nu_{xc}^{hole}(\mathbf{r})$ and ν_{resp}, respectively. In both cases these peaks are a manifestation of the strong localization of the exchange hole on the atom nearest to the reference position $\mathbf{r}$, with as a corollary ''jumping'' of the hole when the reference position crosses the bond midpouint. This localization is due (as is the well-known possibility of orbital localization) to having both bonding and antibonding MOs occupied (which is when we have Pauli repulsion instead of bonding). The bond midpoint maximum in $\nu_{xc}^{hole}(\mathbf{r})$ has been related to the Coulombic tails of the potentials of atom centered localized holes. The large bond midpoint peak of the ''response'' potential ν_{resp} observed for Ne_2 has been characterized as the Pauli repulsion effect, i.e., antibonding orbital occupation, with the help of the approximate expression of Krieger-Li-Iafrate (KLI) for ν_{resp}.

The third component of ν_{xc}, the kinetic component $\nu_{c,kin}$, exhibits a small bond midpoint peak that has been interpreted as the kinetic correlation effect, representing a rapid ''jump'' of the Coulomb correlation hole from one atom to another when the reference electron crosses the bond midpoint.

In the case of N_2, with three electron pair bonds, ν_{xc}^{hole} exhibits a plateau in the bonding region, which reflects the delocalized nature of the corresponding Fermi hole in case of electron pair bonds (only the bonding orbitals occupied). The relatively small bond midpoint peak of ν_{resp} observed for N_2 has been attributed to the Pauli repulsion of the closed $2s$ subshells of the interacting N atoms.

The simple prototype systems Ne_2 and N_2 represent two main types of atomic interaction, covalent bonding on one hand and Pauli repulsion between closed shells on the other hand. One can expect that the accurate potentials ν_{xc} and the exchange-correlation densities ε_{xc} of more complex molecules will display, in different spatial regions, features established for one of these effects or their combination. Furthermore, the study of the Pauli repulsion effect undertaken in this paper is relevant for molecular reactions, since this effect plays an important role in the transition state of a reaction. These problems will be addressed in our further work.

[1] W. Kohn and L. J. Sham, Phys. Rev. **140**, A1133 (1965).
[2] M. A. Buijse, E. J. Baerends, and J. G. Snijders, Phys. Rev. A **40**, 4190 (1989).
[3] O. V. Gritsenko, R. van Leeuwen, and E. J. Baerends, J. Chem. Phys. **101**, 8955 (1994).
[4] P. Süle, O. V. Gritsenko, A. Nagy, and E. J. Baerends, J. Chem. Phys. **103**, 10 085 (1995).
[5] O. V. Gritsenko, R. van Leeuwen, and E. J. Baerends, J. Chem. Phys. **104**, 8535 (1996).
[6] C. O. Almbladh and A. C. Pedroza, Phys. Rev. A **29**, 2322 (1984).
[7] A. C. Pedroza, Phys. Rev. A **33**, 804 (1986).
[8] F. Aryasetiawan and M. J. Stott, Phys. Rev. B **34**, 4401 (1986).
[9] F. Aryasetiawan and M. J. Stott, Phys. Rev. B **38**, 2974 (1988).
[10] A. Nagy and N. H. March, Phys. Rev. A **39**, 5512 (1989).
[11] Q. Zhao and R. G. Parr, Phys. Rev. A **46**, 2337 (1992).
[12] Y. Wang and R. G. Parr, Phys. Rev. A **47**, R1591 (1993).
[13] R. van Leeuwen and E. J. Baerends, Phys. Rev. A **49**, 2421 (1994).
[14] Q. Zhao, R. C. Morrison, and R. G. Parr, Phys. Rev. A **50**, 2138 (1994).
[15] R. C. Morrison and Q. Zhao, Phys. Rev. A **51**, 1980 (1995).
[16] O. V. Gritsenko, R. van Leeuwen, and E. J. Baerends, Phys. Rev. A **52**, 1870 (1995).
[17] O. V. Gritsenko and E. J. Baerends, Phys. Rev. A **54**, 1957 (1996).
[18] O. V. Gritsenko, P. R. T. Schipper, and E. J. Baerends (unpublished).
[19] O. V. Gritsenko, P. R. T. Schipper, and E. J. Baerends, J. Chem. Phys. **107**, 5007 (1997).
[20] P. R. T. Schipper, O. V. Gritsenko, and E. J. Baerends, Phys. Rev. A **57**, 1729 (1998).
[21] V. E. Ingamells and N. C. Handy, Chem. Phys. Lett. **248**, 373 (1996).
[22] D. J. Tozer, V. E. Ingamells, and N. C. Handy, J. Chem. Phys. **105**, 9200 (1996).
[23] J. D. Talman and W. F. Shadwick, Phys. Rev. A **14**, 36 (1976).
[24] D. C. Langreth and J. Mehl, Phys. Rev. B **28**, 1809 (1983).
[25] Y. Wang, J. P. Perdew, J. A. Chevary, L. D. Macdonald, and S. H. Vosko, Phys. Rev. A **41**, 78 (1990).
[26] J. B. Krieger, Y. Li, and G. J. Jafrate, Phys. Rev. A **45**, 101 (1992).

[27] O. V. Gritsenko, R. van Leeuwen, E. van Lenthe, and E. J. Baerends, Phys. Rev. A **51**, 1944 (1995).
[28] R. van Leeuwen, O. V. Gritsenko, and E. J. Baerends, Z. Phys. D **33**, 229 (1995).
[29] O. V. Gritsenko and E. J. Baerends, Theor. Chem. Acc. **96**, 44 (1997).
[30] C. O. Almbladh and U. von Barth, in *Density Functional Methods in Physics*, edited by R. M. Dreizler and J. da Providencia (Plenum Press, New York, 1985), Vol. 123, p. 209.
[31] J. P. Perdew, in *Density Functional Methods in Physics* (Ref. [30]), p. 265.
[32] G. Hunter, Int. J. Quantum Chem. **9**, 237 (1975).
[33] J. B. Krieger, Y. Li, and G. J. Iafrate, Phys. Rev. A **46**, 5453 (1992).
[34] K. Aashamar, T. M. Luke, and J. D. Talman, At. Data Nucl. Data Tables **22**, 443 (1978).
[35] J. D. Talman, Comput. Phys. Commun. **54**, 85 (1989).
[36] E. J. Baerends, in *Cluster Models for Surface and Bulk Phenomena*, Vol. 283 of *NATO Advanced Studies Institute Series B: Physics*, edited by G. Pacchioni, P. S. Bagus, and F. Parmigiani (Plenum Press, New York, 1992); p. 189.
[37] V. R. Saunders and J. H. van Lenthe, Mol. Phys. **48**, 923 (1983).
[38] D. E. Woon and T. H. Dunning, J. Chem. Phys. **103**, 4572 (1995).
[39] M. A. Buijse, thesis, Vrije Universiteit, 1991.
[40] M. A. Buijse and E. J. Baerends, in *Electronic Density Functional Theory of Molecules, Clusters and Solids*, edited by D. E. Ellis (Kluwer Academic Publishers, Dordrecht, 1995), p. 1.
[41] W. L. Luken and D. N. Beratan, Theor. Chim. Acta **61**, 265 (1982).
[42] W. L. Luken, Int. J. Quantum Chem. **22**, 889 (1982).
[43] E. J. Baerends and O. V. Gritsenko, J. Phys. Chem. **101**, 5383 (1997).
[44] A. Rozendaal and E. J. Baerends, Chem. Phys. **95**, 57 (1985).